Solvent and phosphine dependency in the reaction of cis-RuCl$_2$(P–P)$_2$ (P–P = dppm or dppe) with terminal alkynes

Jason M. Lynam *, Tracy D. Nixon, Adrian C. Whitwood

Department of Chemistry, University of York, Heslington, York YO10 5DD, UK

ABSTRACT

Reaction of cis-[RuCl$_2$(dppm)$_2$] (dppm = 1,2-bis(diphenylphosphino)methane) with PhC≡CH and NaPF$_6$ utilising methanol as solvent results in the formation of the η^3-butenynyl complex [Ru(η^3-PhC≡C—C=CHPh)(dppm)$_2$][PF$_6$] in good yield. Similar reactions with Bu^{t}C≡CH and Pr^{n}C≡CH resulted in the corresponding alkyl-substituted complexes and all three of these compounds have been characterised by NMR spectroscopy and X-ray crystallography. The mechanism of this reaction has been probed by employing labelling experiments with both PhC≡CD and PhC≡^{13}CH allowing the identity of possible intermediates in the reaction to be determined. Furthermore, [Ru(η^3-PhC≡C—C=CHPh)(dppm)$_2$][PF$_6$] has been shown to be an effective regio- and stereo-selective catalyst for the dimerisation of PhC≡CH to Z-PhC≡C—CH=CHPh in the absence of solvent. In contrast, no evidence for the formation of alkyne coupling was obtained from the reaction of cis-[RuCl$_2$(dppe)$_2$] (dppe = 1,2-bis(diphenylphosphino)ethane) with PhC≡CH and NaPF$_6$.

1. Introduction

The ability of electron-rich transition-metal complexes to facilitate the isomerisation of terminal alkynes to their vinylidene tautomer is well documented [1] and it is generally accepted that this occurs *via* initial coordination of the alkyne to the metal followed by a formal 1,2-hydrogen shift. The precise mechanism of the 1,2-hydrogen shift appears to be system dependant and is still a focus of both mechanistic [2] and theoretical [3] studies. Two general mechanisms have been proposed for this process the first is based on a discrete metal hydride intermediate, formed by C—H activation of the alkyne followed by hydrogen migration whereas the second involves a concerted 1,2-hydrogen shift.

Vinylidene ligands have been shown to be important synthetic intermediates, this is principally due to the fact that the α-carbon of these ligands are electrophilic and as such are readily attacked even by weak nucleophiles [4]. This phenomenon has been extensively exploited in the catalytic transformation of alkynes [5]. As such a comprehensive understanding of the different factors affecting both the structure and reactivity of vinylidene complexes is an important goal.

We have recently embarked on a programme of research designed to incorporate nucleobases, tethered to alkynes, into the coordination sphere of organometallic complexes [6]. The poor solubility of these materials in many organic solvents has entailed a re-evaluation of many common reactions typically employed to prepare vinylidene complexes. In several cases we have found that changing the solvent has a pronounced effect on the reaction outcome, even when simple alkyl or aryl-substituted alkynes are employed. We now report that the reaction between complexes cis-[RuCl$_2$(P–P)$_2$], (P–P = dppm or dppm) may yield both the previously reported vinylidene species trans-[RuCl(=C=CHR)(P–P)$_2$]$^+$ [7] but also butenynyl species [Ru(η^3-RC≡C—C=CHR)(P–P)$_2$]$^+$, depending on the conditions and phosphine ligand employed. Furthermore, studies using ^{2}D and ^{13}C-labelled alkynes have provided important information about the mechanism of the formation of both compounds.

2. Results and discussion

2.1. Synthetic studies

Treatment of a methanol suspension of cis-[RuCl$_2$(dppm)$_2$] (**1**) with NaPF$_6$ and 2.1 equiv. of PhC≡CH did not result in the expected rapid reaction to give the deep red vinylidene complex trans-[RuCl(=C=CHPh)(dppm)$_2$][PF$_6$] (**2a**) [7]. Instead, over a period of 48 h the solution was observed to turn orange, but a yellow precipitate remained throughout the reaction. The solution was then filtered; the filtrate was shown to contain a number of compounds, including **2a**. The solid residue was extracted with CH$_2$Cl$_2$ to afford a yellow solution from which a bright yellow solid could be isolated in good yield. The ^{31}P{^{1}H} NMR spectra in CD$_2$Cl$_2$ solution of this solid exhibited four resonances for a single new

* Corresponding author. Tel.: +44 (0) 1904 432534; fax: +44 (0) 1904 432516.
E-mail address: jml12@york.ac.uk (J.M. Lynam).

product, **3a**, in an ABMX coupling pattern. Most notable was the large $^2J_{PP}$ coupling constant between resonances at δ −16.21 and δ −26.27 of 320.3 Hz indicating the presence of two phosphorus atoms with a mutually *trans* disposition: a septet resonance was also observed for the PF$_6$ anion. The ^{1}H NMR spectrum of this solution confirmed the asymmetric arrangement of the dppm ligands in **3a**, a further doublet resonance at δ 5.58 ($^4J_{PH}$ = 4.6 Hz), which integrated to one hydrogen atom, was also observed.

Slow diffusion of hexane into a CH$_2$Cl$_2$ solution of **3a** afforded yellow crystals suitable for study by single crystal X-ray diffraction. The structural determination illustrated that **3a** contained a cationic ruthenium centre with a distorted octahedral structure with two dppm ligands (Fig. 1): as expected on the basis of the NMR spectra two of the phosphorus atoms are in a mutually *trans* position. The remaining two coordination sites at the metal are occupied by a diphenyl-substituted η^3-butenynyl ligand which has presumably been formed by a ruthenium-mediated coupling of two molecules of PhC≡CH: the butenynyl ligand exhibits *E*-stereochemistry. The bond lengths and angles for **3a** are presented in Table 1, for convenience the common labelling scheme shown in Table 1 is employed for all of the structures described: details of the data collection and structural refinement are presented in Table 2. The bond lengths within this ligand are consistent with its formulation as an η^3-butenynyl group. For example, the distance between the three ruthenium-bound carbon atoms are 1.248(6) Å (C$_a$–C$_b$) and 1.384 (6) Å (C$_b$–C$_c$). The former is consistent with an alkyne unit bound to the ruthenium: the deviation from a linear geometry (C$_a$–C$_b$–C$_c$ 151.0(4)°) is typical behaviour. The distance between C$_b$–C$_c$ is somewhat longer, but still shorter than that expected for a single bond, which might indicate a contribution to the bonding from resonance form **3ii** (Fig. 2) where the organic ligand binds as a triene. The distance between C$_c$ and C$_d$ {1.330(6) Å} is typical for an uncoordinated alkene. This structure is consistent with the NMR data obtained and, in particular the resonance in the ^{1}H NMR spectrum at δ 5.58 was assigned to the vinyl proton in the butenynyl ligand.

Several other examples of the dimerisation of alkynes within the coordination sphere of ruthenium to give η^3-butenynyl ligands have been reported. For example, Bianchini has demonstrated that reaction of the dihydrogen compound [Ru(H)(H$_2$)(PP$_3$)][BPh$_4$] [PP$_3$ = P(CH$_2$CH$_2$PPh$_2$)$_3$] with PhC≡CH results in the formation of *E*-[Ru(η^3-Ph-C≡C—C=CHPh)(PP$_3$)][BPh$_4$] [8]: a similar product was isolated from the corresponding reaction with Me$_3$SiC≡CH [9]. Insight into how the condensation of the alkynes might occur
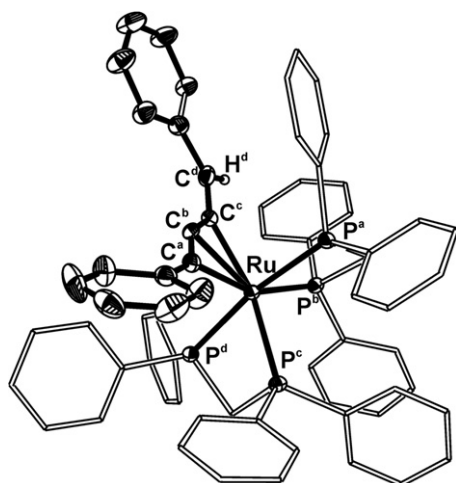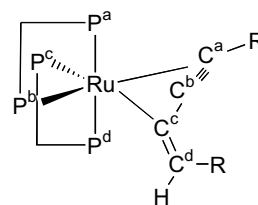

Fig. 1. Structure of the cation of **3a**, thermal ellipsoids, where shown, at the 30% probability level. Hydrogen atoms, except H^d omitted for clarity.

Table 1
Selected bond lengths (Å) and bond angles (°) for **3a**, **3b** and **3c**

	3a	3b[#]	3c
Ru–C^a	2.404(4)	2.404(5)	2.262(4)
Ru–C^b	2.230(4)	2.236(4)	2.215(4)
Ru–C^c	2.156(4)	2.199(4)	2.202(4)
Ru–P^a	2.3350(10)	2.3298(11)	2.3602(10)
Ru–P^b	2.3239(11)	2.3315(11)	2.3277(10)
Ru–P^c	2.3659(10)	2.3672(10)	2.3361(9)
Ru–P^d	2.3845(10)	2.3801(11)	2.3472(10)
C^a–C^b	1.248(6)	1.257(6)	1.301(6)
C^b–C^c	1.384(6)	1.360(6)	1.345(6)
C^c–C^d	1.330(6)	1.317(7)	1.369(6)
C^a–C^b–C^c	151.0(4)	152.4(4)	146.8(4)
C^b–C^c–C^d	136.2(4)	141.8(5)	139.8(4)
Ru–C^c–C^d	147.5(3)	143.5(4)	147.2(3)
P^a–Ru–P^b	71.41(4)	71.69(4)	70.94(3)
P^b–Ru–P^c	94.04(4)	96.33(4)	96.05(3)
P^c–Ru–P^d	70.68(4)	70.55(4)	70.88(3)
P^c–Ru–P^a	102.02(4)	104.57(4)	104.48(3)
P^a–Ru–P^d	170.24(4)	172.53(4)	172.92(3)
P^b–Ru–P^d	102.12(4)	102.83(4)	103.84(3)
C^c–Ru–P^a	89.27(11)	92.62(11)	91.40(12)
C^c–Ru–P^b	97.71(11)	96.23(12)	98.73(12)
C^c–Ru–P^c	165.83(11)	161.21(11)	161.16(13)
C^c–Ru–P^d	98.99(11)	93.04(11)	94.17(12)

The common labelling scheme for all three complexes is adopted as shown above.
[#] Bond length/angles are only reported for the major isomer.

within the coordination sphere of the metal was obtained from the observation that the alkynyl–vinylidene complex [Ru(-C≡CPh)(=C=CHPh)(P{OMe}$_3$)$_4$]$^+$ rearranges in solution to give [Ru(η^3-PhC≡C—C=CHPh)(P{OMe}$_3$)$_4$]$^+$[10]. Other routes to generate these species include the reaction of RuClH(Cyttp) with PhC≡C—C≡CPh to give *anti-mer* and *syn-mer*-[RuCl(η^3-Ph—C≡C—C=CHPh)(Cyttp)] whereas reaction of RuH$_4$(Cyttp) [Cyttp = PhP(CH$_2$CH$_2$CH$_2$P{c-C$_6$H$_{11}$}$_2$)$_2$] with PhC≡CH affords [Ru(-C≡CPh)(η^3-Ph-C≡C—C=CHPh)(Cyttp)] [11,12]. A related compound containing butenynyl and alkynyl ligands, *anti-mer*-[Ru(-C≡CPh)(η^3-Ph-C≡C—C=CHPh)(PNP)], may be prepared from the reaction of *mer*, *trans*-[RuCl$_2$(=C=CHPh)(PNP)] [PNP = Pr^{n}N(CH$_2$CH$_2$PPh$_2$)$_2$] with an excess of LiC≡CPh [13]. Several of these compounds have had their structures determined by single crystal X-ray diffraction [9–13] and the topology of the butenynyl ligand in **3a** is similar to that observed in the related complexes.

The reaction to form **3a** from *cis*-[RuCl$_2$(dppm)$_2$], 2 equiv. of NaPF$_6$ and 2.1 equiv. of PhC≡CH although selective was somewhat slow and therefore efforts were made to optimise the synthesis. By simply increasing the amount of PhC≡CH employed in the reaction to 10 equiv. **3a** could be isolated in excellent yield after 16 h.

In order to gauge the applicability of the synthetic procedure to aliphatic alkynes the reaction of **1** with NaPF$_6$ in MeOH and 10 equiv. of Bu^{t}C≡CH was investigated. This afforded a mixture of [Ru(η^3-Bu^{t}C≡C—C=CHBu^t)(dppm)$_2$][PF$_6$] (**3b**) and *trans*-[RuCl(=C=CHBu^t)(dppm)$_2$][PF$_6$] (**2b**). The vinylidene side-product could be eliminated by increasing the quantity of Bu^{t}C≡CH used in the reaction to 50 equiv. In a similar fashion, performing the reaction with 50 equiv. of Pr^{n}C≡CH resulted in the formation of [Ru(η^3-Pr^{n}C≡C—C=CHPr^n)(dppm)$_2$][PF$_6$] (**3c**) in good yield. The ^{31}P{^{1}H} NMR spectra of **3b** and **3c** exhibited the characteristic

Table 2
Crystal data and refinement for complex **3a**, **3b** and **3c**

	3a	3b	3c
Empirical formula	$C_{66.25}H_{55.50}Cl_{0.50}F_6P_5Ru$	$C_{62}H_{63}F_6P_5Ru$	$C_{60.50}H_{60}ClF_6P_5Ru$
Formula weight	1239.25	1178.04	1192.45
T (K)	112(2)	110(2)	110(2)
Wavelength (Å)	0.71073	0.71073	0.71073
Crystal system	Monoclinic	Monoclinic	Triclinic
Space group	$P2(1)/n$	$P2(1)/c$	$P\bar{1}$
a (Å)	12.1261(13)	13.2173(15)	11.0461(13)
b (Å)	24.302(3)	17.822(2)	13.1283(16)
c (Å)	19.830(2)	23.718(3)	19.875(2)
α (°)	90	90	85.602(2)
β (°)	101.035(2)	93.356(2)	88.018(2)
γ (°)	90	90	74.061(2)
V (Å)^3	5735.7(10)	5577.1(11)	2762.9(6)
Z	4	4	2
D_{calc} (Mg m^{-3})	1.435	1.403	1.433
Absorption coefficient (mm^{-1})	0.498	0.484	0.536
$F(000)$	2538	2432	1226
Crystal size (mm)	$0.12 \times 0.10 \times 0.10$	$0.15 \times 0.13 \times 0.09$	$0.41 \times 0.15 \times 0.08$
Theta range for data collection (°)	1.83–25.09	1.72–25.02	1.03–28.40
Index ranges	$-14 \leqslant h \leqslant 14, -28 \leqslant k \leqslant 28,$ $-23 \leqslant l \leqslant 23$	$-15 \leqslant h \leqslant 15, -21 \leqslant k \leqslant 21,$ $-28 \leqslant l \leqslant 28$	$-14 \leqslant h \leqslant 14, -17 \leqslant k \leqslant 17,$ $-26 \leqslant l \leqslant 26$
Reflections collected	45698	43926	13570
Independent reflections [R_{int}]	10178 [0.0777]	9819 [0.0809]	13570 [R(int) = 0.0321]
Completeness (to theta)°	99.6 (to 25.09)	99.7 (to 25.02)	97.8 (to 28.40)
Absorption correction	Semi-empirical from equivalents	Semi-empirical from equivalents	Semi-empirical from equivalents
Data/restraints/parameters	10178/1/731	9819/6/761	13570/6/780
Goodness-of-fit (GOF) on F^2	1.026	1.023	1.029
Final R indices [$I > 2\sigma(I)$]	$R_1 = 0.0478, wR_2 = 0.1064$	$R_1 = 0.0470, wR_2 = 0.1038$	$R_1 = 0.0581, wR_2 = 0.1559$
R indices (all data)	$R_1 = 0.0764, wR_2 = 0.1184$	$R_1 = 0.0816, wR_2 = 0.1162$	$R_1 = 0.0654, wR_2 = 0.1611$
Largest difference peak and hole (e Å^{-3})	0.697 and −0.751	0.882 and −0.609	2.575 and −0.814

ABMX spin system shown by **3a**. Complexes **3b** and **3c** appear to be formed as a mixture of isomers as a minor set of resonances with a
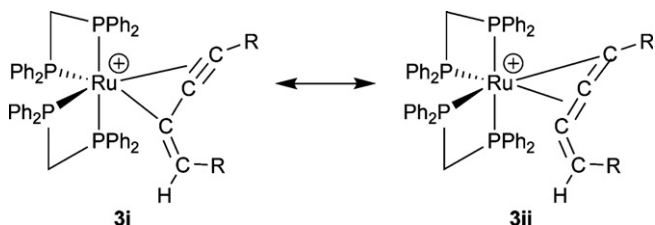

Fig. 2. Possible resonance forms that may be used to describe the structure of butenynyl complexes.

similar ABMX spin system are observed in both cases. We assign this second isomer to simply be the Z-isomer of the complex. The structures of **3b** and **3c** were unambiguously determined by single crystal X-ray diffraction (see Figs. 3 and 4, respectively). In both cases, however, a small number of orange crystals were also obtained from the reaction mixtures on standing in CD_2Cl_2 which were shown to be *trans*-[RuCl$_2$(dppm)$_2$] · 2CD$_2$Cl$_2$, **4** · 2CD$_2$Cl$_2$, by single crystal X-ray diffraction (see Supplementary Information). An examination of the NMR spectra of the crude reaction mixture illustrated that **4** was indeed a minor product of the reaction.
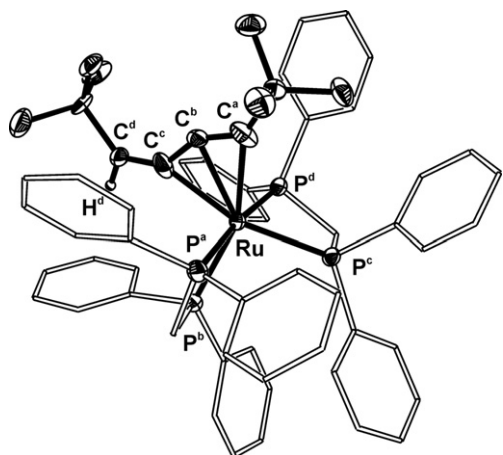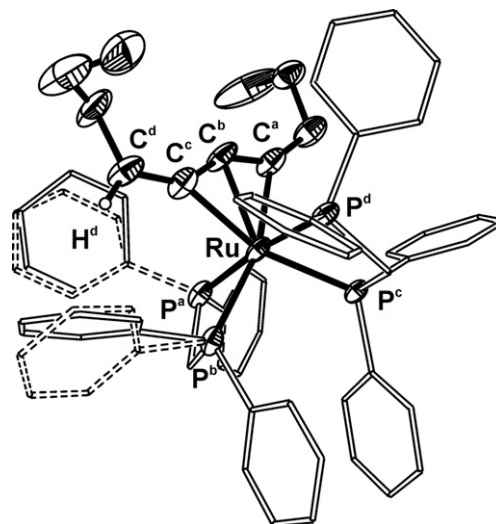

Fig. 3. Structure of the more abundant cation of **3b**, thermal ellipsoids, where shown, at the 30% probability level. Hydrogen atoms, except H^d omitted for clarity.

Fig. 4. Structure of the cation of 6, thermal ellipsoids, where shown, at the 30% probability level. Hydrogen atoms, except H^d, omitted for clarity. Two of the phenyl groups are disordered with a 50:50 occupancy, these are indicated by the dotted rings.

The gross topology of complexes **3a–c** are essentially identical: in each case the double bond exhibits *E*-stereochemistry. Interestingly, complex **3b** crystallised as a mixture of forms in a 80:20 ratio, the structure of the major component is shown in Fig. 3. The minor component has the butenynyl ligand rotated by 180° relative to the Ru(dppm)$_2$ framework. Some disorder is also observed in **3c**: two of the phenyl rings on a dppm ligand show different orientations. As shown in Table 1, the bond lengths and angles within complexes **3a** and **3b** are, to within statistical significance, identical. In contrast, the structure of **3c** exhibits some differences to these two complexes. In particular the triple bond of the butenynyl unit appears to be interacting more strongly with the metal in **3c**. Notably the Ru–C$_a$ distance is shorter {2.262(4) Å} than the corresponding distance in either **3a** {2.404(4) Å} or **3b** {2.404(5) Å} and the "triple bond" of the butenynyl (C$_a$-C$_b$) ligand is longer {1.301(6) Å} in **3c** than in either **3a** {1.248(6) Å} or **3b** {1.257(6) Å}. This is as would be expected on the basis of the Dewar–Chatt–Duncanson model if the metal is interacting more strongly with the butenynyl ligand in **3c** than in the other two complexes. In a similar vein the formal "single bond"(C$_b$–C$_c$) with the butenynyl unit is shorter in **3c** 1.345(6) Å than in **3a** {1.384(6) Å} and the Ru–C$_c$ bond in **3c** is longer {2.202(4) Å} than in **3a** {2.156(4) Å}. These results may be interpreted in terms of a greater contribution to the bonding in **3c** from resonance form **3ii** (Fig. 2) than in **3a** or **3b**. We have rationalised this effect on the basis of the relative steric demands of the Pr^n and Ph groups. The reduced steric bulk and additional conformation flexibility of the Pr^n groups in **3c** compared to either the Ph (in **3a**) or Bu^t (in **3b**) ensures that the butenynyl ligand in **3c** may interact more strongly with the ruthenium in this case resulting in the observed geometric changes.

2.2. Mechanistic studies

Given the somewhat unexpected formation of the η^3-butenynyl complexes the mechanism and factors affecting their formation were investigated. Therefore, the original reaction, reported by Dixneuf, to form **2a** was re-examined. Treatment of a dichloromethane solution of **1** with NaPF$_6$ and PhC≡CH resulted in the formation of a deep red solution that, as expected, contained **2a** as the major product. A close examination of the ^{31}P{^{1}H} NMR spectra of the crude reaction mixture illustrated that small quantities of **3a** were also present. The reaction was repeated and monitored by ^{31}P{^{1}H} NMR spectroscopy over a period of several weeks. During this time the resonances for **3a** increased in intensity at the expense of the peak for **2a**. A series of other species were also observed during the formation of **3a**, the most abundant, **5a**, exhibited resonances as δ 19.9 (dd, $^2J_{PP}$ = 39.0 and 12.9 Hz), δ 16.0 (ddd, $^2J_{PP}$ = 400.9 Hz, 39.0 Hz and 17.5 Hz), δ −8.3 (dd, $^2J_{PP}$ = 54.8 Hz and 17.5 Hz) and δ −21.6 (ddd, $^2J_{PP}$ = 400.9 Hz, 54.8 Hz and 12.9 Hz). Importantly, the ^{31}P{^{1}H} NMR spectra of the reaction mixture showed that **5a** was formed in substantial quantities before **3a**. Repeating the same reaction in CD$_3$OD also resulted in the formation of **3a**, however due to the poor solubility of both **2a** and **3a** in this solvent medium the reaction only proceeded when frequently sonicated.

The alkynyl complex *trans*-[Ru(−C≡CPh)Cl(dppm)$_2$] (**6a**) may also act as a precursor for **3a**. Treatment of samples of **6a** (which contained small amounts of the bis-alkynyl complex *trans*-[Ru(−C≡CPh)$_2$(dppm)$_2$] (**7a**) [14]) in MeOH solution with NaPF$_6$ and PhC≡CH resulted in the formation of **2a** and **3a** in approximately equal amounts. In contrast, when the reaction was performed in CH$_2$Cl$_2$ only **2a** was formed over the same time period.

Further mechanistic insight into these processes was gained through a series of isotopic labelling studies. The reactions to form both **2a** (in CH$_2$Cl$_2$) and **3a** (in MeOH) were repeated with PhC≡CD. In both cases the ^{1}H NMR spectrum showed no evidence for deuterium incorporation into the final product demonstrating that the vinylidene proton possesses considerable acidity. In the presence of a proton source (the OH proton in MeOH or adventitious water in CH$_2$Cl$_2$) a rapid exchange may occur via **6a**. It is important to note that this is in contrast to the data obtained by Grotjahn who demonstrated that the vinylidene proton in complexes RhCl(=C=CH$_2$)L$_2$ (L = phosphorus ligand) did not under deuterium exchange with D$_2$O [2b]. The difference in behaviour may simply be rationalised by considering that the cationic nature of **2a** would promote the acidity of the vinylidene proton compared to the neutral rhodium-based system.

Corresponding reactions between **1** and PhC≡^{13}CH in CH$_2$Cl$_2$ and MeOH afforded *trans*-[RuCl(=^{13}C=CHPh)(dppm)$_2$][PF$_6$], ^{13}C-**2a**, and [Ru(η^3-Ph-C≡^{13}C−^{13}C=CHPh)(dppm)][PF$_6$], ^{13}C$_2$-**3a**, respectively. The availability of these labelled materials allowed
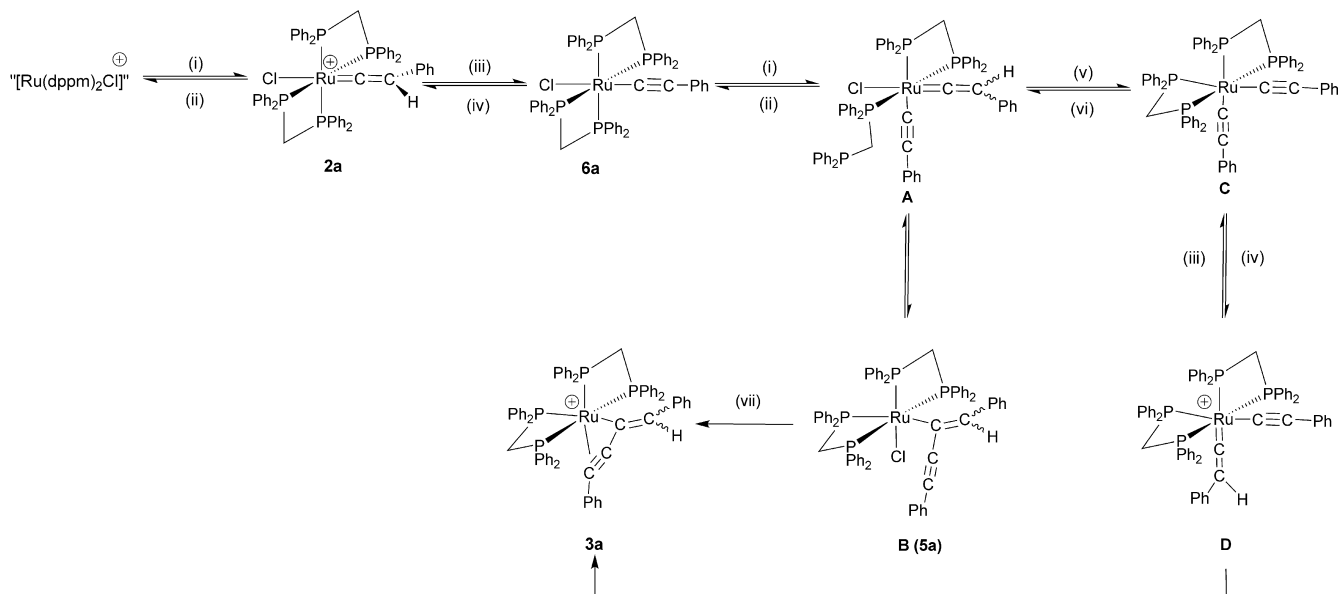
Scheme 1. (i) + PhC$_2$H, (ii) − PhC$_2$H, (iii) − H$^+$, (iv) + H$^+$, (v) − HCl, (vi) + HCl, (vii) − Cl$^-$.

us to further study the interactions of alkynes with the ruthenium centre in more detail.

The reaction of ^{13}C-**2a** with one equivalent of PhC≡CH in CD$_2$Cl$_2$ solution resulted in a decrease in the intensity of the doublet resonance in the ^{31}P{^{1}H} NMR spectrum ($^2J_{PC}$ = 12.2 Hz) and the appearance of a singlet due to unlabelled **2a**. An identical experiment involving the reaction of **2a** with PhC≡^{13}CH resulted in the formation of some ^{13}C-**2a**. These results demonstrate that the vinylidene ligand in **2a** is labile and may readily undergo degenerate alkyne exchange.

These studies also provided some further information about the structure of possible intermediates in the formation of **3a** from **2a**. Although the precise nature of these species could not be unambiguously determined, the presence of the ^{13}C label revealed several important structural features. In both the reaction of **2a** with PhC≡^{13}CH and ^{13}C-**2a** with PhC≡CH a *quartet* resonance was observed at δ 363.1 ($^2J_{PC}$ = 15.5 Hz) in the ^{13}C{^{1}H} NMR spectra. The implication of the quartet multiplicity of this resonance is that a complex with a vinylidene ligand *cis* to three PPh$_2$ is present, inferring the presence of a pendant PPh$_2$ group. The ability of dppm ligands to act in this hemi-labile manner in ruthenium(II) complexes has been previously reported [15]. In addition, the ^{31}P{^{1}H} NMR spectrum exhibited the same resonances for **5a** as described above and a series of overlapping peaks for ^{13}C-**5a**: with the resonance at δ 19.9 showing an additional doublet coupling $^2J_{PC}$ coupling of 86.0 Hz: the three other resonances all exhibiting doublet couplings to the ^{13}C-labelled nucleus of 15.3 Hz, implying a structure with one phosphorus *trans* to an organic ligand formed from PhC≡CH, and the other three *cis*.

In an attempt to determine the fate of the two alkyne groups in the final butenynyl product a sample of ^{13}C-**2a** was treated with PhC≡CH in MeOH solution. The ^{13}C{^{1}H} NMR spectrum of the product recorded in CD$_2$Cl$_2$ solution indicated that ^{13}C incorporation had occurred at both C$_b$ and C$_c$ to give ^{13}C(C$_b$)-**3a** and ^{13}C(C$_c$)-**3a** respectively in almost equal amounts. No evidence of ^{13}C-incorporation at both positions to give ^{13}C$_2$-**3a** was obtained. A similar reaction between **6a** and PhC≡^{13}CH in MeOH resulted in the formation of a complex mixture containing ^{13}C$_2$-**3a** and smaller amounts of ^{13}C-^{13}C(C$_c$)-**3a** and ^{13}C(C$_b$)-**3a**.

In order to explain our findings we propose the mechanism shown in Scheme 1. The reaction of *cis*-RuCl$_2$(dppm)$_2$ with NaPF$_6$ results in the creation of a vacant coordination site at the metal: bind of an alkyne to this site results in the formation of the vinylidene ligand **2a**. This step is reversible as we have observed exchange between free and coordinated alkyne. Given that no deuterium label is incorporated into **2a** when PhC≡CD is used we propose that **2a** is in rapid equilibrium with **6a**. Subsequent reaction of **6a** with PhC≡CH may then be envisaged to result in the formation of intermediate **A**, containing a pendant phosphine group and a vinylidene ligand. The structure of **A** is consistent with the observation of a quartet resonance at δ 363.1 in the ^{13}C{^{1}H} NMR spectrum. Combination of acetylide and vinylidene ligands, which in previous studies has been proposed to be the key C–C bond formation step, will then lead to intermediate **B**, which contains an η^1-bound butenynyl ligand. The structure of **B** is consistent with the spectroscopic data obtained for **5a**. Finally, loss of chloride would result in the formation of **3a**.

Although this mechanism is consistent with many of the experimental observations, it does not provide a rationale for the fact that the reaction of ^{13}C-**2a** with PhC≡CH results in the formation of both ^{13}C(C$_b$)-**3a** and ^{13}C(C$_c$)-**3a**. In addition the lack of deuterium incorporation in the product is not readily explained. Therefore, the presence of the symmetric intermediate **C** is proposed, formed by loss of HCl from **A**. This provides a convenient explanation for both the lack of deutereium incorporation in the product and the scrambling of positions of the ^{13}C-label as both acetylide ligands are now equiva-

lent and the reversible protonation could occur at either. In this case the equilibrium between **A** and **C** must be more rapid than the subsequent formation of **C**. Related *bis*-alkynyl complexes have been prepared and have been shown to undergo protonation to give η^3-enyl complexes [16,17]. In addition, protonation of **C** could also lead to the cationic complex **D** without re-addition of Cl$^-$. Combination of vinylidene and alkynyl ligands would then afford **3a** directly. We have not obtained any evidence for the presence of compounds related to **C** and **D** in the reaction mixture, but this does not preclude their role in the formation of **3a**.

The pronounced solvent effects observed in these reactions may be rationalised in several ways. It is apparent that the reaction of **1** with PhC≡CH to give **2a** is rapid and the subsequent reaction to give **3a** is slower. Therefore, when CH$_2$Cl$_2$ is employed as solvent, the high solubility of **1** in this medium ensures that a rapid formation of **2a** occurs consuming 1 equiv. of alkyne. In contrast, **1** is far less soluble in MeOH therefore the formation of **2a** is far slower and as such the relative concentration of PhC≡CH in solution higher, hence the observation of **3a** as the major product in this case. Although this provides an explanation for the initial observation of **3a**, it does not provide a basis to rationalise the results obtained from the reactions of **6a** with PhC≡CH and MeOH. One plausible explanation for these results is that methanol may simply promote halide or phosphorus dissociation from the vinylidene and alkynyl complexes in a more effective manner than dichloromethane, therefore creating a vacant coordination site and permitting binding of a second molecule of PhC≡CH. The possibility of methanol simply acting as a mild acid to promote the formation of **3a** was also considered. Although this possibility cannot be explicitly ruled out, the reaction of **2a** with PhC≡CH in presence of HBF$_4$ · OEt$_2$ did not appear to enhance the formation of **3a**.

2.3. Catalytic dimerisation of PhC≡CH

As several related butenynyl complexes[8,9,16–21] have been proposed as intermediates in the catalytic dimerisation of alkynes, we were intrigued to discover if **3a** could promote the dimerisation of PhC≡CH [22]. This indeed proved to be the case. Reaction of **3a** with 100 equiv. of PhC≡CH in MeOH at room temperature resulted in the formation of a deep yellow solution, from which it was possible to re-isolate the starting ruthenium complex. The predominant organic product from the reaction was *Z*-PhC≡CCH=CHPh: some *E*-PhC≡CCH=CHPh could be observed. The overall yield of organic products was very poor (<10%). A series of studies were under taken in order to optimise the reaction conditions. The best results were obtained when the procedure was performed in neat PhC≡CH at 110 °C. Under these conditions quantitative conversion to *Z*-PhC≡CCH=CHPh was observed over a 24 h period only trace amounts (*ca.* 1%) of the *E*-isomer were obtained: mass spectrometry also indicated that trace amounts of trimeric products were formed. When these conditions were employed, ^{31}P{^{1}H} spectroscopy showed that only small amounts of **3a** remained after the reaction, this material showed considerably diminished catalytic activity when the reaction was repeated. Presumably under these more forcing conditions the complex decomposed in the absence of substrate.

Performing catalytic dimerisation using **3a** in neat PhC≡CD or with PhC≡^{13}CH results in quantitative formation of PhC≡CCD=CDPh and PhC≡^{13}C^{13}CH=CHPh, respectively. In contrast, reaction of **3a** with 100 equiv. of PhC≡CD in MeOH solution resulted in little or no deuterium incorporation as shown by NMR spectroscopy. As in the mechanistic study described above, it is clear that in the presence of a protic medium, H/D exchange occurs rapidly.

From a mechanistic viewpoint, the catalytic process may occur *via* protonation of **3a** with PhC≡CH to give *Z*-PhC≡CCH=CHPh
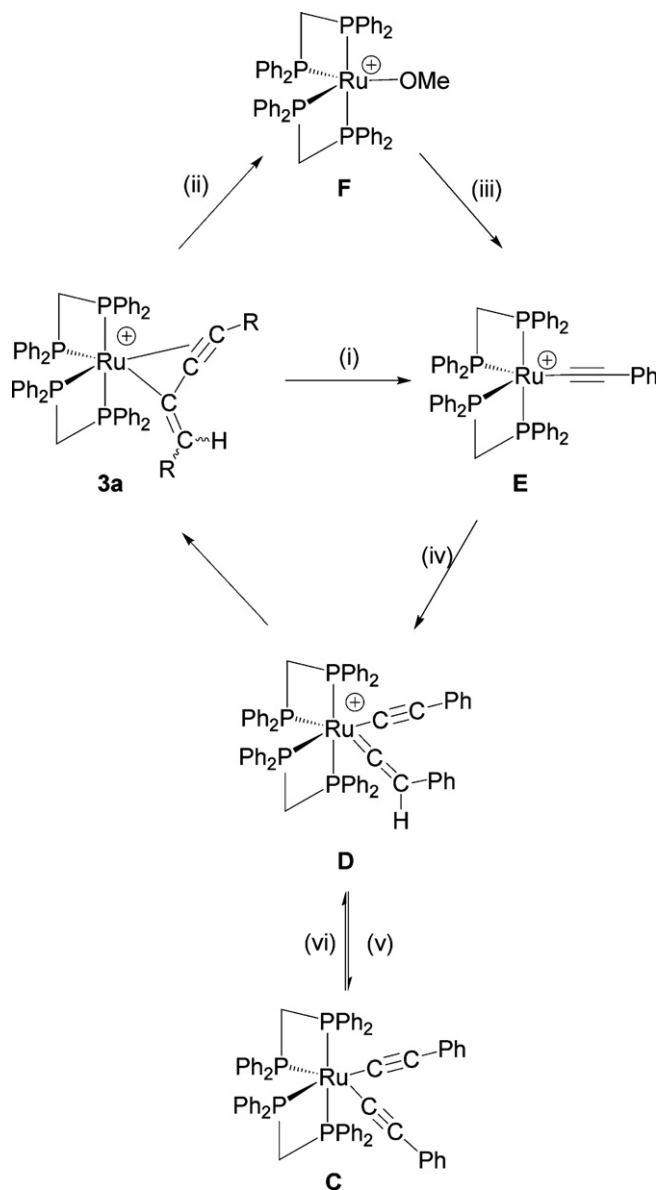
Scheme 2. (i) + PhC$_2$H, − PhC≡CCH=CHPh. (ii) + MeOH, − PhC≡CCH=CHPh. (iii) + PhC$_2$H, − MeOH. (iv) PhC$_2$H. (v) − H$^+$. (vi) + H$^+$.

{Scheme 2, step (i)} and the sixteen electron alkynyl species **E**: this process may of course be assisted by the dissociation of a phosphorus atom, or the triple bond of the butenynyl ligand from the metal centre creating a vacant site for alkyne coordination. Although our results support the mechanism involving dissociation of a phosphorus ligand, it is important to note that Bianchini has demonstrated that reaction of *E*-[Ru(η^3-Ph-C≡C–C=CHPh)(PP$_3$)]$^+$ with CO results in the formation of *E*-[Ru(η^1-{Ph-C≡C}–C=CHPh)(CO)(PP$_3$)]$^+$ [8], although as our study of the related dppe system (*q.v.*) demonstrates that the phosphorus-containing ligand appears to have a considerable influence in the chemistry of these compounds.

The assembly of the butenynyl ligand may then occur in a similar manner (**E → D → 3a**): the lack of deuterium incorporation when the reaction is performed in MeOH gives further credence to the intermediacy of **C** in this process. For this process to account for the total lack of deuterium incorporation it is clear that alkyne coordination, H/D exchange and alkyne dissociation must be rapid in comparison to the subsequent loss of the enyne. It is also feasi-

ble that protonation of **3a** by the solvent MeOH (if employed) to afford *Z*-PhC≡CCH=CHPh and the methoxide complex **F** may also be a viable mechanistic pathway in this solvent. Reaction of **F** with PhC≡CH would afford MeOH and **E**, which may then lead to the regeneration of **3a**.

2.4. Reactions of cis-[RuCl$_2$(dppe)$_2$]

In light of the new insights observed with the dppm system we elected to probe the related species, *cis*-[RuCl$_2$(dppe)$_2$] [7,23], to see if exhibits similar chemistry. In the event, we discovered that there is a significant difference in the reactivity of these two systems and that the addition of a single extra CH$_2$ linker in the phosphine ligand backbone has a pronounced effect on the outcome of the reaction. Treatment of a methanol solution of *cis*-[RuCl$_2$(dppe)$_2$], with NaPF$_6$ and 2.1 equiv. of PhC≡CH resulted in the rapid formation of a red solution. A ^{31}P{^{1}H} NMR spectrum of the reaction mixture illustrated that no species analogous to **3a** was formed, but *trans*-[RuCl(=C=CHPh)(dppe)$_2$][PF$_6$] (**8a**) was a component of the reaction mixture. Furthermore, when the reaction was repeated with 100 equiv. of PhC≡CH no evidence for the formation of any products resulting from alkyne dimerisation was obtained.

The difference in behaviour between the dppm and dppe-containing systems may be explained in terms of the different size of the bite angles in the dppm and dppe ligands. The smaller bite angle of dppm presumably means that the ruthenium centre is more open to reaction with a second equivalent of PhC≡CH thus allowing the subsequent dimerisation to occur. An alternative explanation is that the hemi-lability of the dppm (which forms a four-membered chelate ring) ligand, which serves to create a vacant coordination site at the metal, is not exhibited by dppe (a five membered chelate ring) hence prohibiting the coordination of a second molecule of alkyne. Presumably the four-membered ring exhibited by dppm is considerably more strained than the five-membered dppe analogue hence providing a rationale for the differing reactivity of the two systems.

2.5. Conclusions

In conclusion, we have demonstrated that the change in reaction solvent and the nature of the phosphorus-containing ligand may have a pronounced effect on the outcome of the reaction of metal complexes with alkynes. This effect might be due to the poor solubility of **1** in MeOH or alternatively, the favouring of ligand dissociation in this solvent over CH$_2$Cl$_2$.

The η^3-butenynyl complex, **3a**, is a catalyst for the highly regioselective dimerisation of PhC≡CH. Considering the facile synthesis of **3a** and the high selectivity this complex exhibits for the dimerisation of PhC≡CH in a solvent-less medium, this system offers several advantages for the synthesis of enynes. We are currently exploring the scope of this reaction, and in particular the apparent enhanced reactivity of the dppm-containing system, with regard to the oligomerisation of a range of functionalised alkynes.

3. Experimental

All experimental procedures were performed under an atmosphere of nitrogen or argon using standard Schlenk Line and Glove Box techniques. All solvents were purified by distillation under argon prior to use from appropriate drying agents (MeOH from Mg/I$_2$, CH$_2$Cl$_2$ from CaH$_2$ and hexane and Et$_2$O from Na/benzophenone). The CD$_2$Cl$_2$ used for NMR experiments was dried over CaH$_2$ and degassed with three freeze–pump–thaw cycles. The solvent was then vacuum transferred into NMR tubes fitted with PTFE Young's taps.

cis-[RuCl$_2$(dppm)$_2$] (**1**) [24], cis-[RuCl$_2$(dppe)$_2$] (**7**) [24], trans-[RuCl(=C=CHPh)(dppm)$_2$][PF$_6$] (**2a**) [7] and trans-[Ru(-C≡CPh)Cl(dppm)$_2$] (**6a**) [7], were prepared as described previously. NaPF$_6$, (Fluorochem) dppe, PhC≡^{13}CH ^{n}PrC≡CH and ^{t}BuC≡CH, (Aldrich) and dppm (Acros Organics) were used without further purification. PhC≡CH was purchased from Alfa Aesar and passed through a short alumina plug prior to use. PhC≡CD was prepared by deprotonation of PhC≡CH with LiBu^n and quenching of the reaction with D$_2$O. Deuterium incorporation was confirmed by mass spectrometry.

NMR spectra were acquired on a Bruker AMX 300 (Operating Frequencies ^{1}H 300.13 MHz, ^{31}P 121.40 MHz, ^{13}C 76.98 MHz) ^{31}P and ^{13}C spectra were recorded with proton decoupling. The aromatic region of the ^{13}C{^{1}H} NMR spectra could not be adequately deconvoluted even with the aid of HMQC spectra. Mass spectrometry measurements were performed on a Thermo-Electron Corp. LCQ Classic (ESI) instrument.

3.1. Synthesis of **3a**

PhC≡CH (150 μl, 1.25 mmol) was added to a stirred suspension of cis-[RuCl$_2$(dppm)$_2$] (120 mg, 0.125 mmol) and NaPF$_6$ (4 mg, 0.250 mmol) in methanol (10 ml). The reaction mixture was stirred for 16 h during which time an orange solution was formed. The solution was filtered and the residue extracted with CH$_2$Cl$_2$ (10 ml) that, after removal of the solvent in vacuo, yielded a yellow solid that was washed with Et$_2$O (2 × 10 ml). Samples of **3a** obtained in this manner were generally pure enough to use in further reactions, although the complex could be further purified by crystallisation from CH$_2$Cl$_2$/hexane. Yield 76%. NMR Spectra CD$_2$Cl$_2$, ^{1}H δ 4.23 (1H, m, C**H**$_2$), 4.56 (1H, m, C**H**$_2$), 5.01 (2H, m, C**H**$_2$), 5.58 (1H, d, C^d**H**, $^4J_{PH}$ = 4.6 Hz), 6.30–7.89 (aromatic region). ^{31}P{^{1}H} δ –143.90 (septet, $^1J_{PF}$ 711.0 Hz, PF$_6^-$), –26.39 (ddd, 320.4 Hz, 46.9 Hz, 27.5 Hz), –16.34 (ddd, 320.4 Hz, 32.2 Hz, 26.3 Hz), –13.26 (ddd, 32.6 Hz, 27.6 Hz, 9.7 Hz), –0.07 (ddd, 46.2 Hz, 26.2 Hz, 10.2 Hz). ^{13}C{^{1}H} δ 41.43 (at, $^2J_{PC}$ = 23.5 Hz, Ph$_2$P**C**H$_2$), 44.61 (at, $^2J_{PC}$ = 24.1 Hz, Ph$_2$P**C**H$_2$), 52.03 (s, **C**^{b}), 109.11 (d, $^2J_{PC}$ = 23.0 Hz, **C**^{a}). Mass Spectrum (ESI) m/z 1073.2 M$^+$, 905 {Ru(dppm)$_2$(C$_3$)-H}$^+$ or Ru(dppm)(P$_2$C$_{25}$H$_{21}$)(C$_3$)$^+$, 869 Ru(dppm)$_2^+$, 689 Ru(dppm)(PhC$_4$HPh)$^+$. IR (CH$_2$Cl$_2$)ν = 3683 cm^{-1} (br), 3061 cm^{-1} (br), 1605 cm^{-1} (br), 1484 cm^{-1} (br, w), 1436 cm^{-1} (s), 1097 cm^{-1} (br). Elemental analysis for C$_{66}$H$_{55}$P$_5$F$_6$Ru.0.25CH$_2$Cl$_2$ calc. C, 64.21, H, 4.51, Found C, 63.99, H, 4.60%.

3.2. Synthesis of **3b**

Complex **3b** could be prepared in an identical manner to that described for **3a** using the same quantities of solvent, cis-[RuCl$_2$(dppm)$_2$] (120 mg, 0.125 mmol) and NaPF$_6$. In order to obtain high yields a large excess of Bu^{t}C≡CH (0.77 ml, 6.25 mmol) was employed. Yield 73%. NMR Spectra CD$_2$Cl$_2$, ^{1}H δ 0.55 (9H, s, C{C**H**$_3$}$_3$), 0.83 (9H, s, C{C**H**$_3$}$_3$), 4.37 (3H, m, C**H**$_2$ and C^d**H**, d, $^4J_{PH}$ = 5.1 Hz), 4.56 (1H, m, C**H**$_2$), 4.85 (1H, m, C**H**$_2$), 5.01 (1H, m, C**H**$_2$), 6.61–7.90 (aromatic region). ^{31}P{^{1}H} δ –143.90 (septet, $^1J_{PF}$ 711.0 Hz, PF$_6^-$), –27.06 (ddd, 329.5 Hz, 42.4 Hz, 29.0 Hz), –20.99 (ddd, 329.5 Hz, 36.2 Hz, 28.3 Hz), –16.51 (ddd, 36.2 Hz, 28.4 Hz, 7.7 Hz), –1.77 (ddd, 42.2 Hz, 28.5 Hz, 7.7 Hz). ^{13}C{^{1}H} δ 30.13 (s, C{C**H**$_3$}$_3$), 32.38 (s, C{C**H**$_3$}$_3$), 37.61(s, **C**{CH$_3$}$_3$), 37.66 (s, **C**{CH$_3$}$_3$), 42.17 (m, Ph$_2$P**C**H$_2$), 45.59 (m, Ph$_2$P**C**H$_2$), 48.28 (s, **C**^{b}), 117.41 (d, $^2J_{PC}$ = 25.5 Hz, **C**^{a}). Minor Isomer ^{31}P{^{1}H} δ –25.34 (ddd, 321.7 Hz, 45.0 Hz, 31.4 Hz), –19.22 (ddd, 321.7 Hz, 43.9 Hz, 24.0 Hz), –5.75 (ddd, 43.8 Hz, 31.0 Hz, 29.7 Hz), 0.25 (ddd, 45.0 Hz, 29.1 Hz, 24.1 Hz). Mass Spectrum (ESI) m/z 1033.29 M$^+$, 905 {Ru(dppm)$_2$(C$_3$)-H}$^+$ or Ru(dppm)(P$_2$C$_{25}$H$_{21}$)(C$_3$)$^+$. IR (CH$_2$Cl$_2$)ν = 3684 cm^{-1} (br), 3066 cm^{-1} (br) 2962 cm^{-1} (br), 1605 cm^{-1} (br), 1485 cm^{-1} (br,

w), 1438 cm^{-1} (s), 1096 cm^{-1} (br). Elemental analysis for C$_{62}$H$_{63}$P$_5$F$_6$Ru C 63.21, H 5.39, Found C, 62.46, H, 5.46.

3.3. Synthesis of **3c**

Complex **3c** could be prepared in an identical manner to that described for **3a** using the same quantities of solvent, cis-[RuCl$_2$(dppm)$_2$] (120 mg, 0.125 mmol) and NaPF$_6$ and Pr^{n}C≡CH (0.62ml, 6.25 mmol), of Pr^{n}C≡CH. Crystals suitable for study by X-ray diffraction were grown from a concentrated CD$_2$Cl$_2$/hexane solution of **3c**. Yield 60%. NMR Spectra, CD$_2$Cl$_2$, ^{1}H δ 0.73 (3H, t, 6.9 Hz, C**H**$_3$CH$_2$), 0.78 (3H, t, 7.5 Hz, C**H**$_3$CH$_2$), 1.00 – 1.21 (2H, m, C**H**$_2$), 1.27 (2H, sept, 7.5 Hz, CH$_3$C**H**$_2$CH$_2$), 2.00 (2H, m, C**H**$_2$), 2.21 (2H, sept, 6.9 Hz, CH$_3$C**H**$_2$CH$_2$), 4.27 (2H, m, C**H**$_2$), 4.75 (1H, m, C**H**$_2$), 4.80 (1H, d, $^4J_{PH}$ = 5.0 Hz, C^d**H**), 5.00 (1H, m, C**H**$_2$), 6.57–7.89 (aromatic region). ^{31}P{^{1}H} δ – 143.90 (septet, $^1J_{PF}$ 711.0 Hz, PF$_6^-$), –25.82 (ddd, 336.0 Hz, 46.3 Hz, 29.4 Hz), –12.87 (ddd, 336.2 Hz, 31.3 Hz, 26.4 Hz), –12.48 (ddd, 38.9 Hz, 29.4 Hz, 9.8 Hz), –0.35 (ddd, 45.9 Hz, 26.1 Hz, 10.2 Hz). ^{13}C{^{1}H} δ 14.00 (s, **C**H$_3$), 14.55 (s, **C**H$_3$), 23.36 (s, **C**H$_2$), 25.38 (d, J_{PC} = 2.6 Hz, **C**H$_2$), 27.93 (s, **C**H$_2$), 42.42 (at, $^2J_{PC}$ = 25.2 Hz, Ph$_2$P**C**H$_2$), 42.50 (t, J_{PC} = 2.6 Hz, **C**H$_2$), 42.98 (d, $^2J_{PC}$ = 5.06 Hz, **C**^{b}), 44.10 (at, $^2J_{PC}$ = 24.1 Hz, Ph$_2$P**C**H$_2$), 107.56 (dt, $^2J_{PC}$ = 23.9 Hz, 3.2 Hz, **C**^{a}). Minor product ^{31}P{^{1}H} δ – 25.37 (ddd, 321.8 Hz, 45.7 Hz, 31.9 Hz), –19.18 (ddd, 321.8 Hz, 44.0 Hz, 24.2 Hz), –5.73 (ddd, 43.9 Hz, 30.7 Hz, 29.5 Hz), 0.25 (ddd, 45.1 Hz, 28.9 Hz, 24.1 Hz). Mass Spectrum (ESI) m/z 1005.26 M$^+$, 905 {Ru(dppm)$_2$(C$_3$)-H}$^+$ or Ru(dppm)(P$_2$C$_{25}$H$_{21}$)(C$_3$)$^+$. IR (CH$_2$Cl$_2$)ν = 3053 cm^{-1} (br), 2958 cm^{-1} (br), 1484 cm^{-1} (br, w), 1435 cm^{-1} (s), 1096 cm^{-1} (br). Elemental analysis for C$_{60}$H$_{59}$P$_5$F$_6$Ru calculated. C, 62.66, H, 5.17; Found C, 62.25, H, 5.11%.

3.4. Catalytic studies

All catalytic reactions were performed in a sealed ampoule fitted with a PTFE Young's Tap. In a typical solventless procedure, the ampoule was charged with a stir bar, complex **3a** (20 mg, 0.016 mmol) and PhC≡CH (180 μl, 1.60 mmol). The tube was sealed and heated to 110 °C for 24 h with stirring. After cooling the resulting residue was extracted with Et$_2$O to afford Z-PhC≡CCH=CHPh (133 mg, 79%). If required the organic product could be further purified by passage down a flash silica column. The reaction could be performed in an identical manner by replacing **3a** with **1** and NaPF$_6$: in this case poor E/Z selectivity was observed.

3.5. Details of X-ray diffraction analysis

Crystals of complexes **3a–c** were grown by slow diffusion of hexane into a CD$_2$Cl$_2$ solution of the appropriate compound. Details of the collection and refinement are presented in Table 2. Diffraction data were collected at 110 K on a Bruker Smart Apex diffractometer with Mo Kα radiation (λ = 0.71073 Å) using a SMART CCD camera. Diffractometer control, data collection and initial unit cell determination was performed using "SMART" [25]. Frame integration and unit-cell refinement software was carried out with "SAINT+" [26]. Absorption corrections were applied by SADABS (v2.03, Sheldrick). Structures were solved by direct methods using SHELXS-97[27] and refined by full-matrix least squares using SHELXL-97 [28]. All non-hydrogen atoms were refined anisotropically. Hydrogen atoms were placed using a "riding model" and included in the refinement at calculated positions. The butenynyl ligand in **3b** is disordered about two positions, the relative occupancy of each being allowed to refine, the result of which is a 80:20 occupancy. In the structure of **3c** two of the phenyl groups were disordered and were refined using two-site models. In both cases the relative occupancy refined to 1:1. There was evidence of twinning of the crystal. The TwinRotMat routine in PLATON [29] was used to partially resolve this problem.

There remained two sites of significant density in the difference map. These are translations of the position of the Ru in the "*ac*" plane and are presumably due to the presence of smaller crystals related to the main crystal by translation along the "*ac*" plane.

Acknowledgements

Appendix A. Supplementary material

CCDC 637644, 637645, 637646 and 637647 contain the supplementary crystallographic data for **3a**, **3b**, **3c** and **4**.2CD$_2$Cl$_2$. These data can be obtained free of charge from The Cambridge Crystallographic Data Centre via www.ccdc.cam.ac.uk/data_request/cif.

Supplementary data associated with this article can be found, in the online version, at doi:10.1016/j.jorganchem.2008.06.021.

References

[1] (a) .M.I. Bruce, Chem. Rev. 91 (1991) 197;
(b) H. Werner, J. Organomet. Chem. 475 (1994) 45;
(c) Y. Wakatsuki, J. Organomet. Chem. 689 (2004) 4092;
(d) M.C. Puerta, P. Valerga, Coord. Chem. Rev. 193–195 (1999) 977.
[2] (a) D. B Grotjahn, X. Zeng, A.L. Cooksy, J. Am. Chem. Soc. 128 (2006) 2798;
(b) D.B. Grotjahn, X. Zeng, A.L. Cooksy, W.S. Kassel, A.G. DiPasquale, L.N. Zakharov, A.L. Rheingold, Organometallics 26 (2007) 3385;
(c) M.J. Cowley, J.M. Lynam, J.M. Slattery, Dalton Trans. (in press) doi:10.1039/b806358c.
[3] F. De Angelis, A. Sgamellotti, N. Re, Dalton Trans. (2004) 3225.
[4] C. Bianchini, J.A. Casares, M. Peruzzini, A. Romerosa, F. Zanobini, J. Am. Chem. Soc. 118 (1996) 4585.
[5] (a) B.M. Trost, M.U. Frediksen, M.T. Rudd, Angew. Chem., Int. Ed. 44 (2005) 6630;
(b) C. Bruneau, P.H. Dixneuf, Angew. Chem., Int. Ed. 45 (2006) 2176;
(c) C. Bruneau, P.H. Dixneuf, Acc. Chem. Res. 32 (1999) 311;
(d) M. Tokunaga, T. Suzuki, N. Koga, T. Fukushima, A. Horiuchi, Y. Wakatsuki, J. Am. Chem. Soc. 123 (2001) 11917;
(e) D.B. Grotjahn, D.A. Lev, J. Am. Chem. Soc. 126 (2004) 12232;
(f) D.B. Grotjahn, C.D. Incarvito, A.L. Rheingold, Angew. Chem., Int. Ed. 40 (2001) 3884.
[6] (a) H. Hamidov, J.C. Jeffery, J.M. Lynam, Chem. Commun. (2004) 1364;
(b) M.J. Cowley, J.M. Lynam, A.C. Whitwood, Dalton Trans. (2007) 4427.
[7] D. Touchard, P. Haquette, N. Pirio, L. Toupet, P.H. Dixneuf, Organometallics 12 (1993) 3132.
[8] C. Bianchini, C. Bohanna, M.A. Esteruelas, P. Frediani, A. Meli, L.A. Oro, M. Peruzzini, Organometallics 11 (1992) 3837.
[9] C. Bianchini, M. Peruzzini, F. Zanobini, P. Frediani, A. Albinati, J. Am. Chem. Soc. 113 (1991) 5453.
[10] G. Albertin, S. Antoniutti, E. Bordignon, F. Cazzaro, S. Ianelli, G. Pelizzi, Organometallics 14 (1995) 4114.
[11] G. Jia, A.L. Rheingold, D.W. Meek, Organometallics 8 (1989) 1378.
[12] G. Jia, D.W. Meek, Organometallics 10 (1991) 1444.
[13] C. Bianchini, P. Innocenti, M. Peruzzini, A. Romerosa, F. Zanobini, Organometallics 15 (1996) 279.
[14] During the preparation of these **3a** was also observed as a minor product.
[15] (a) J. Ruiz, V. Riera, M. Vivanco, J. Chem. Soc., Dalton Trans. (1995) 1069;
(b) J. Ruiz, M.E.G. Mosquera, V. Riera, J. Organomet. Chem. 527 (1997) 35.
[16] T. Rappert, A. Yamamoto, Organometallics 13 (1994) 4984.
[17] C. Bianchini, P. Frediani, D. Masi, M. Peruzzini, F. Zanobini, Organometallics 13 (1994) 4616.
[18] C. Bianchini, A. Meli, M. Peruzzini, F. Vizza, Organometallics 9 (1990) 1146.
[19] C. Slugovc, K. Mereiter, E. Zobetz, R. Schmid, K. Kirchner, Organometallics 15 (1996) 5275.
[20] J.Q. Wang, A.K. Dash, J.C. Berthet, M. Ephritikhine, M.S. Eisen, Organometallics 18 (1999) 2407.
[21] J.-H. Lee, K.G. Caulton, J. Organometal. Chem. 693 (2008) 1664.
[22] (a) For related catalytic systems see for example: M. Nishiura, Z. Hou, J. Mol. Cat. A. 213 (1994) 101;
(b) M. Nishiura, Z. Hou, Y. Wakatsuki, T. Yamaki, T. Miyamoto, J. Am. Chem. Soc. 125 (2003) 1184;
(c) C. Yang, S.P. Nolan, J. Org. Chem. 67 (2002) 591;
(d) C.G.J. Tazelaar, S. Bambirra, D. van Leusen, A. Meetsma, B. Hessen, J.H. Teuben, Organometallics 23 (2004) 936;
(e) H. Katayama, M. Nakayama, T. Nakano, C. Wada, K. Akamastu, F. Ozawa, Macromolecules 37 (2004) 13;
(f) T. Hirabayashi, S. Sakaguchi, Y. Ishii, Adv. Synth. Cat. 347 (2005) 872;
(g) X. Chen, P. Xue, H.H. Y Sung, I.D. Williams, M. Peruzzini, C. Bianchini, G. Jia, Organometallics 24 (2005) 4330.
[23] D. Touchard, P. Haquette, S. Guesmi, L. Le Pichon, A. Daridor, L. Toupet, P.H. Dixneuf, Organometallics 16 (1997) 3640.
[24] B. Chaudret, G. Commenges, R. Poilblanc, J. Chem. Soc., Dalton Trans. (1984) 1635.
[25] Smart Diffractometer Control Software (v5.625), Bruker-AXS, Bruker AXS GmbH, Karlsruhe, Germany.
[26] SAINT+ (v6.22) Bruker AXS, Bruker AXS GmbH, Karlsruhe, Germany.
[27] G.M. Sheldrick, SHELXS-97, Program for the Solution of Crystal Structures, Universität Göttingen, 1997.
[28] G.M. Sheldrick, SHELXL-97, Program for the Refinement of Crystal Structures, Universität Göttingen, 1997.
[29] A.L. Spek, PLATON; Molecular Geometry and Plotting Program, University of Utrecht, The Netherlands, 1997.